

**Atomic and electronic structure of an unreconstructed polar MgO(111) thin film on Ag(111)**

Manabu Kiguchi, Shiro Entani, and Koichiro Saiki

*Department of Complexity Science & Engineering, Graduate School of Frontier Sciences, The University of Tokyo, 7-3-1 Hongo, Bunkyo-ku, Tokyo 113-0033, Japan*

Takayuki Goto and Atsushi Koma

*Department of Chemistry, Graduate School of Science, The University of Tokyo, 7-3-1 Hongo, Bunkyo-ku, Tokyo 113-0033, Japan*  
(Received 16 March 2003; published 5 September 2003)

Atomic and electronic structures of a polar surface of MgO formed on Ag(111) was investigated by using reflection high-energy electron-diffraction, Auger-electron spectroscopy, electron energy-loss spectroscopy (EELS), and ultraviolet photoemission spectroscopy (UPS). A rather flat unreconstructed polar MgO(111)  $1 \times 1$  surface could be grown by alternate adsorption of Mg and O<sub>2</sub> on Ag(111). The stability of the MgO(111) surface was discussed in terms of interaction between Ag and Mg atoms at the interface and charge state of the surface atoms. EELS of this surface did not show a band-gap region, and finite density of states appeared at the Fermi level in UPS. These results suggest that a polar MgO(111) surface was not an insulating surface but a semiconducting or metallic surface.

DOI: 10.1103/PhysRevB.68.115402

PACS number(s): 79.60.Jv, 61.14.Hg, 68.55.-a

**I. INTRODUCTION**

Polar surfaces have attracted wide attention not only for fundamental science but also for technological applications, because several interesting properties, such as novel catalytic activity and two-dimensional electron system, are expected for the polar surface. Figure 1 shows the atomic geometry of nonpolar (100) and polar (111) faces of rocksalt crystals schematically. The (111) surface consists of only one atomic species, either cations or anions, while the (100) surface consists of the same number of cations and anions. In a rocksalt structure crystal, each atom is surrounded by six atoms of different species. The coordination number decreases to 5 for atoms on a (100) surface, while it changes drastically to 3 for atoms on a (111) surface. Therefore, surface energy of the (111) face is much higher than that of the (100) face, which makes the (111) surface unstable.<sup>1</sup> In other words, alternate stacking of cation and anion layers forms a dipole layer along the [111] direction [Fig. 2(a)]. Accumulation of the dipole layers would produce a macroscopic electric field, which causes the appearance of a flat (111) surface to be quite unpreferable in the rocksalt structure compounds and the flat (111) surface does not occur in nature.

From a theoretical viewpoint, the macroscopic electric field in the polar surface can be canceled either by surface reconstruction or by reduction of effective charge of the surface layer. According to Wolf, the polar (111) surface of rocksalt crystals would be stable under an octapole termination, which leads to the formation of a  $2 \times 2$  reconstruction on the (111) surface<sup>1</sup> [Fig. 2(b)]. On the other hand, Tsukada and Hoshino pointed out that the change in charge state of surface atoms could stabilize the (111) surface of rocksalt structure compounds.<sup>2</sup> If the charge of top atoms is reduced to half of the bulk atoms, the macroscopic electric field would not appear.

Under these backgrounds, several attempts to grow the polar surface of rocksalt structure compounds have been performed so far.<sup>3</sup> Metal oxides have been extensively studied

to create crystals or thin films having (111) surfaces. For a NiO(111) surface,  $p(2 \times 2)$  reconstruction was found, and the surface was determined to be a single Ni termination with double steps by the measurement of grazing-incidence x-ray diffraction.<sup>4</sup> The unreconstructed surface is stabilized by some adsorbates. Langell and Berrie reported that the NiO(111) surface is stabilized by OH adsorbates and that desorption of the hydroxyl changes the surface to a thermodynamically more stable NiO(100).<sup>5</sup> Stabilization by impurities was found also for Pb and Si on NiO(111).<sup>6</sup>

In contrast with the surface of single crystals, the electrostatic energy does not reach exorbitant values for the small thickness of a film [Fig. 2(c)]. When the thin film is grown on a metal substrate, further reduction of energy could come from the image charge induced in the supporting metal surface. Ventrice *et al.* have studied the growth of NiO on Au(111) by low-energy electron diffraction (LEED) and scanning tunneling microscopy (STM), and obtained a 6-ML-thick stable  $p(2 \times 2)$  reconstructed NiO(111) film.<sup>7</sup> For a FeO(111) thin film, interesting results were reported by Koike and Furukawa.<sup>8</sup> They obtained the FeO(111)  $p(2 \times 2)$  surface by oxidizing Fe(110) and measured the polarization of secondary electrons emitted from the FeO(111) surface. Ferromagnetic ordering was found for the FeO(111)  $p(2 \times 2)$  surface, although FeO itself was an antiferromagnetic material with the Néel temperature of 198 K. They thought that the ferromagnetic ordering comes from the re-

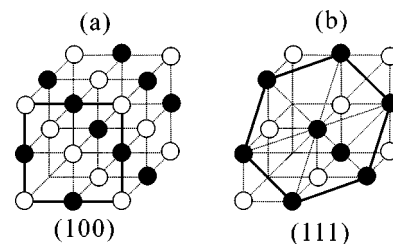


FIG. 1. Atomic geometry of the nonpolar (100) and polar (111) faces of a rocksalt crystal.

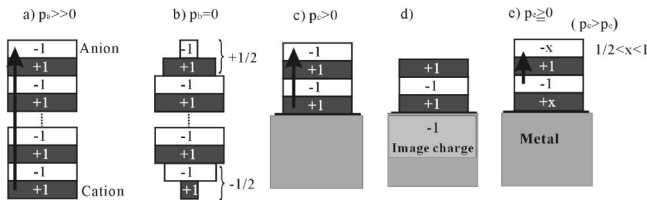


FIG. 2. Charge distribution and resulting dipole moments ( $p$ ) for (111) surfaces discussed. The numbers in the layers refer to the typical charge per atom. (a) Thick (111) film; (b) reconstructed surface, only one-fourth and three-fourth of the lattice positions are occupied for the first and the second layer, respectively; (c) neutral 4-ML-thick (111) film, and (d) 3-ML-thick (111) film on a metal substrate neutralized by an image charge; and (e) neutral 4-ML-thick (111) film, the charge of the top and bottom atoms reduces to  $x$  of the bulk atoms ( $1/\leq x \leq 1$ ). The dipole moment of (e) case is smaller than that of (c) case.

construction of a polar FeO(111) surface to reduce the large electrostatic surface energy. On the other hand, the relaxation, that is, the decrease in interlayer spacing, was observed for the FeO(111) grown on Pt (111).<sup>9</sup> In this case, the layer by layer growth was limited to a maximum of 2.5 ML (where ML stands for monolayers).

Thus, although the (111) surface of rocksalt structure oxides has been studied by many groups, there have been few studies on unreconstructed adsorbate-free (111) surfaces of a rocksalt structure until now. Furthermore, the electronic structure of the polar surface has not been clear. In the present study, we have examined growth of a MgO thin film on Ag(111) by supplying Mg and O, alternately. MgO has a rocksalt structure with a lattice constant of 4.21 Å, while Ag has a fcc structure with a lattice constant of 4.09 Å. As the lattice misfit of MgO to Ag is only  $-2.9\%$ , the first Mg layer is expected to become a template for the growth of the MgO film along the [111] direction. The commensurate bonding between Mg and Ag atoms at the interface might help alternate stacking of Mg and O layers, leading to a flat (111) surface. Actually, we have observed a rather streak RHEED pattern, implying formation of a flat (111) MgO surface. We have characterized the grown surface by using electron energy-loss spectroscopy (EELS) and ultraviolet photoemission spectroscopy (UPS) and discussed stabilization mechanism of the polar surface.

## II. EXPERIMENT

The experiments were performed in a custom-designed ultrahigh-vacuum (UHV) system with a base pressure of  $2 \times 10^{-8}$  Pa. A mechanically and electrochemically polished Ag(111) surface was cleaned by repeated cycles of Ar<sup>+</sup> sputtering and annealing at 900 K. After repeated preparation cycles, a sharp RHEED pattern was observed, and no contamination was detected by Auger-electron spectroscopy (AES). A MgO film was grown by alternate adsorption of Mg and O<sub>2</sub> on Ag(111) at substrate temperature of 300 K. First, 1-ML (2 Å) Mg was deposited by evaporating high purity (99.98%) Mg onto Ag(111). The growth rate was monitored using a quartz crystal oscillator. The Mg film was

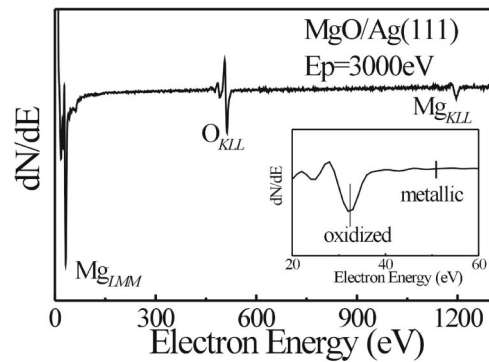


FIG. 3. Auger-electron spectra for the 10-ML-thick MgO film on Ag(111). The primary-electron energy is 3 keV.

dosed with 10-L O<sub>2</sub>. Real-time observation of the crystallinity and orientation of films was done by RHEED. Surface compositions and the electronic structure of the grown films were investigated *in situ* by AES, EELS, and UPS. The analyses were performed with a double pass CMA (PHI 15-255G) in the analysis chamber. Adoption of a pulse counting detector reduced the probing electron current down to 1 nA, which reduced surface damage as much as possible.

## III. RESULTS

### A. Heteroepitaxial growth of MgO on Ag(111)

Figure 3 shows the Auger spectrum of the 10-ML-thick MgO film grown on Ag(111). Disappearance of the Ag LMM Auger peak (351 eV) indicated that the grown MgO film covered the Ag(111) substrate completely because the inelastic mean free path of 351 eV electron was around 1 nm. The chemical state of Mg atoms of the MgO film was known by the energy of the Mg LMM Auger peak, because the energy of the Mg LMM Auger peak is 45 eV and 32 eV for metallic Mg and MgO, respectively.<sup>10</sup> The energy of the Mg LMM Auger peak was 32 eV for the grown MgO film, showing that Mg was completely oxidized. The stoichiometry of the MgO film was also examined by the ratio of the Mg KLL Auger peak intensity to the O KLL Auger peak intensity. Considering the Auger-electron emission probabilities,<sup>11</sup> the ratio of the amount of Mg to that of O was  $1:0.92 \pm 0.18$ ,<sup>12</sup> supporting the idea that a stoichiometric MgO film was grown on Ag(111).

Figure 4 shows the typical sequence of RHEED pattern during the growth at a substrate temperature of 300 K. The incident electron beam was parallel to the  $[1\bar{1}0]$  azimuth of the substrate. The result of RHEED patterns indicated that the MgO film grew heteroepitaxially on Ag(111). The epitaxial orientation of the MgO film was determined to be  $(111)_{\text{MgO}} // (111)_{\text{Ag}}$  and  $[1\bar{1}0]_{\text{MgO}} // [1\bar{1}0]_{\text{Ag}}$ . The half-order streaks did not appear during the growth, showing that the  $(1 \times 1)$  unreconstructed MgO(111) film was grown on Ag(111). Streaks in RHEED patterns indicated that a rather flat (111) surface could be obtained. The RHEED pattern became blurred with increasing film thickness, suggesting that a thick MgO(111) film was unstable.

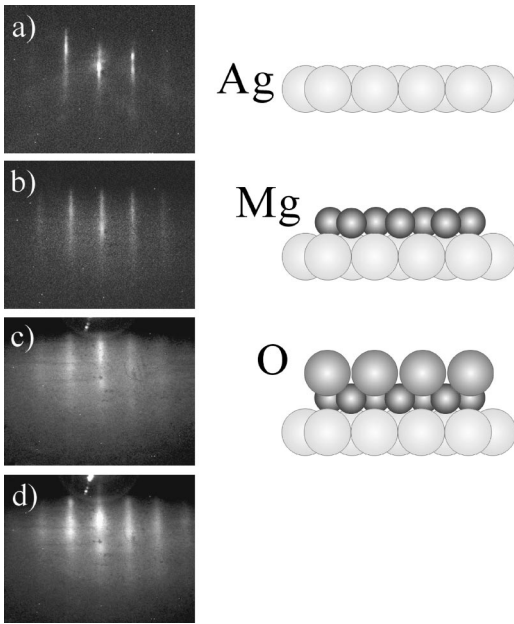


FIG. 4. A typical sequence of RHEED patterns and schematic models during the growth of the MgO film on Ag(111) at a substrate temperature of 300 K. (a) Ag(111), (b) 1-ML Mg/Ag(111), (c) 2-ML MgO/Ag(111), (d) 10-ML MgO/Ag(111). The incident beam was parallel to the  $[1\bar{1}0]$  azimuth of the Ag(111).

The in-plane lattice constant of the MgO(111) film was calculated from the spacing between streaks in the RHEED pattern. For the 10-ML-thick MgO(111)/Ag(111), the in-plane lattice constant was determined to be  $3.28 \pm 0.03 \text{ \AA}$ ,<sup>12</sup> which was +10% larger than that of the bulk one ( $2.97 \text{ \AA}$ ). The in-plane lattice constant was  $3.25 \pm 0.03 \text{ \AA}$  for the 2-ML-thick film and did not change with film thickness, indicating that the expansion was uniform throughout the epitaxial layer. The increase of the in-plane lattice constant leads to reduction of the surface electron density, which might help a decrease in the electrostatic energy of the MgO(111) film.

### B. Stability of the $(1 \times 1)$ MgO(111) film on Ag(111)

Having established the existence of the  $(1 \times 1)$  unreconstructed MgO(111) film on Ag(111), we should discuss why this structure is stable in spite of the previously mentioned arguments on the instability of a polar surface of ionic crystals.<sup>1</sup> We think that the stabilization of the  $(1 \times 1)$  unreconstructed MgO(111) film can be explained in terms of interaction between Ag and Mg atoms at the interface and charge state of surface atoms.

In the previous study, a single crystalline MgO(100) film grew heteroepitaxially on Ag(100) by evaporating MgO congruently from an electron-beam evaporator (EB).<sup>13</sup> On Ag(111), however, a MgO film could not grow heteroepitaxially by EB. Heteroepitaxial growth of a single crystalline MgO film was achieved by alternate adsorption of Mg and  $O_2$  on Ag(111). These facts indicate that the strong interaction between Mg and Ag atoms plays a decisive role in stabilizing the  $(1 \times 1)$  MgO(111) film. The free energy of the

interface ( $E_{inter}$ ) is smaller for the case with coherent Mg-Ag bonds as compared with the case, in which fine particles with thermodynamically more stable  $\{100\}$  faces grow on Ag(111) without coherent Mg-Ag bonds. The structure of the grown film is determined to minimize the sum of the electrostatic energy of the film ( $E_{electro}$ ) and  $E_{inter}$ . Here, we should note that  $E_{electro}$  of a (111) film does not reach exorbitant values for ultrathin films [see Fig. 2(c)], because  $E_{electro}$  is proportional to the film thickness. Therefore, the gain in interaction between Mg and Ag overcomes the disadvantage of the electrostatic energy, and the  $(1 \times 1)$  unreconstructed MgO(111) film is grown on Ag(111). In addition to the strong interaction with Mg atoms, the Ag substrate plays another important role for stabilization of the MgO(111) film. The MgO film was prepared by alternate adsorption of Mg and  $O_2$ . Therefore, the film is unstable due to breakdown of charge neutrality [Fig. 2(d)], when the film thickness is an odd number (Mg top). On the metal substrate, however, the image charge is induced in a metal, helping stabilization of the film with odd layers.

Besides the strong interaction between Mg and Ag atoms at the interface, the stabilization of MgO(111) can be explained in terms of charge state. Due to the reduction of the coordination number, Madelung potential largely decreases for the surface  $O^{2-}$  on the (111) surface. The binding energy of the  $2p$  band, thus, decreases for the surface  $O^{2-}$  and the Fermi level might be located in the  $2p$  band. In such a case, electrons flow out of the upper valence states of the surface  $O^{2-}$ , and the charge of the surface  $O^{2-}$  is reduced. The charge of  $Mg^{2+}$  at the interface would also decrease to keep the film neutral [Fig. 2(e)]. The decrease in the charge reduces a macroscopic electric field, and the instability of the film should be remedied. That is the second point to stabilize the polar MgO(111) film on Ag(111). Here we should note that the reduction in charge of surface  $O^{2-}$  leads to reduction of Madelung potential. Therefore, the amount of the charge transfer is determined under the condition in which both Madelung potential and the charge of surface  $O^{2-}$  are self-consistent. Tsukada and Hoshino studied the O-terminated MgO(111) surface by DV- $X\alpha$  calculations, and revealed that the charge of the top and bottom atoms is reduced to half of the bulk atoms.<sup>2</sup> When the charge of the surface atom is reduced to half of the bulk atoms, the macroscopic electric field would not appear, irrespective of the film thickness. In the present study, a thick MgO(111) film could not be grown on Ag(111), implying that the charge of the topmost O atoms did not reduce to half of the bulk one.

Finally, we would discuss the surface reconstruction of the MgO(111) film. Since the surface energy of a  $\{100\}$  face is lower than that of a  $\{111\}$  face in rocksalt structure compounds,  $\{100\}$  faces are expected to appear for growth normal to the (111) face. In case of NaCl/GaAs(111), triangular pyramids with three exposed  $\{100\}$  faces grow on the substrate.<sup>3,14</sup> As discussed in Introduction, a  $p(2 \times 2)$  reconstructed NiO(111) film is grown on Au(111),<sup>7</sup> and the  $p(2 \times 2)$  structure corresponds to the smallest triangular pyramids surrounded by  $\{100\}$  faces. Here, we should note that both films were grown by congruent evaporation of NiO or NaCl at the substrate temperatures higher than 420 K. There-

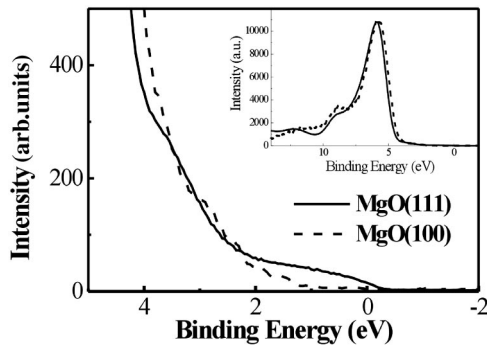


FIG. 5. UPS of the polar MgO(111) surface taken with He I source. Spectra of the MgO(100) surface is shown for comparison.

fore, the grown film forms in a thermodynamically stable structure. In the present case, however, we have grown a metastable flat MgO(111) film by alternate adsorption of Mg and O<sub>2</sub> at 300 K. Once a flat (111) film is formed on Ag(111), activation energy is needed to change the metastable (111) film into stable triangular pyramids surrounded by {100} faces. Therefore, the flat unreconstructed (111) MgO film remains in a metastable form on Ag(111).

### C. Electronic structure of MgO(111)

As we could prepare the unreconstructed polar MgO(111) surface, the electronic structure of this surface was investigated by EELS and UPS, comparing with that of a nonpolar MgO(100) surface.<sup>13,15</sup> Absence of Ag LMM Auger peak in the 10-ML MgO(111)/Ag(111) assures that EELS and UPS probe the MgO film with influences of the substrate negligible, because their probing depth is smaller than or equal to that of AES.

Figure 5 shows UPS spectrum for the MgO(111) surface measured with a He I (21.2 eV) source. For comparison, the spectrum of the 10-ML-thick MgO(100) film on Ag(100) is included in the same figure. The main features for MgO(111) were almost similar to those for MgO(100) except around the Fermi level. For MgO(100), there were no density of states (DOS) near the Fermi level, while an appreciable DOS appeared in the region from 2 eV to the Fermi level for MgO(111). These finite DOS at the Fermi level did not originate from metallic Mg, since component of metallic Mg was not observed in AES. Furthermore, we have revealed that the finite DOS at the Fermi level disappeared even for the incompletely oxidized film in the previous study.<sup>16</sup> Therefore, the finite DOS at Fermi level did not originate from metallic Mg or the incompletely oxidized Mg, the surface states of MgO(111). The UPS results suggested that the polar MgO(111) surface was a metallic surface.

Figure 6 shows the EELS of the MgO(111) surface measured with primary electron energy of 60 eV. For comparison, spectrum of the MgO(100) surface is also shown in the figure. The structure above 7 eV for MgO(111) was almost similar to that of MgO(100), showing that a stoichiometric MgO film grew on Ag(111).<sup>13,15</sup> On the other hand, difference appears in the structure below 5 eV between MgO(100) and (111). In contrast with MgO(100), the clear band-gap

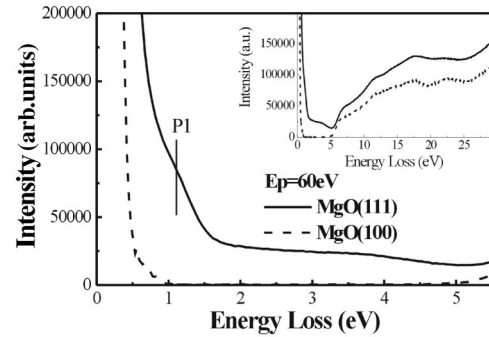


FIG. 6. EEL spectra of the polar MgO(111) surface (line). The primary-electron energy was 60 eV. Spectra of MgO(100) surface is shown for comparison (dotted line).

region was not observed for MgO(111). In addition, the tail of the elastic peak became larger and a new peak (*p1*) appeared at 1.2 eV, indicating existence of the inelastically scattered electrons with small loss energy.<sup>17</sup> Since the AES signal indicative of Mg metal was not observed at all, the tail or the new peak did not originate from Mg aggregates in the MgO film.

Due to the low growth temperature and the significant mismatch between the substrate and the oxide lattice, the film may contain a significant concentration of defects. Therefore, the spectroscopic features could be due to emission from defect states in the MgO(111) film. Defective MgO surfaces have been studied by a variety of techniques such as UPS, EELS, theoretical calculation, etc. In EELS of defective MgO surfaces, sharp peaks are observed at 2.3 eV and 5 eV, which are attributed to Mg vacancy (*V* center) and O vacancy (*F* center), respectively. Sharp structures are also observed for MgO powders by diffuse reflectance spectra, and these structures at 5.8 and 4.6 eV have been attributed to ions with fourfold and threefold ligand coordination.<sup>18</sup> On the other hand, such sharp peaks were not observed in the EELS of MgO (111) below 5 eV. Recently, we have revealed that metal induced gas states (MIGS) were formed at the insulator-metal interface.<sup>19</sup> Since the new states of the MgO(111) film were observed independently of the film thickness, the states did not originate from MIGS. Therefore, the structure below 5 eV could be assigned to the excitation of electrons in the unfilled band derived from O 2p, or the excitations of newly appearing electronic states on the (111) surface.

The UPS and EELS results suggested that the MgO(111) surface was not an insulating surface but a semiconducting or metallic surface. This electronic structure of the MgO(111) surface can be explained in terms of Madelung potential as discussed in the preceding section. Compared to the binding energy of isolated ions, the binding energy of Mg<sup>2+</sup> 3s orbital decreases, and the binding energy of O<sup>2-</sup> 2p orbital increases by the Madelung potential in a crystal phase. Because of the decrease in the coordination number, the Madelung potential largely decreases for the (111) surface, compared with the (100) surface. Therefore, the band gap is reduced and the MgO(111) surface changes into a

semiconductor or metallic surface. However, a possibility of a certain new electronic state characteristic of the (111) surface cannot be excluded.

#### IV. CONCLUSIONS

Heteroepitaxial growth of MgO on Ag(111) has been investigated by RHEED, AES, UPS, and EELS. The flat unreconstructed polar MgO(111) surface was obtained on Ag(111) by alternate adsorption of Mg and O<sub>2</sub> at substrate temperature of 300 K. The EELS and UPS of the (111) sur-

face were different from those of the (100) surface. For MgO(111), a clear band-gap region was not observed in EELS, while finite density of states appeared in UPS, implying that the MgO(111) surface was a semiconducting or metallic surface.

#### ACKNOWLEDGMENTS

The authors are grateful for the financial support of the Grant-in-Aid from Ministry of Education, Culture, Sports, Science and Technology of Japan.

- 
- <sup>1</sup>D. Wolf, Phys. Rev. Lett. **68**, 3315 (1992).  
<sup>2</sup>M. Tsukada and T. Hoshino, J. Phys. Soc. Jpn. **51**, 2562 (1982).  
<sup>3</sup>K. Saiki, A. Goda, and A. Koma, Jpn. J. Appl. Phys., Part 2 **36**, L55 (1997).  
<sup>4</sup>A. Barbier, C. Mocuta, H. Kuhlbeck, K.F. Peters, B. Richter, and G. Renaud, Phys. Rev. Lett. **84**, 2897 (2000).  
<sup>5</sup>M.A. Langell and C.L. Berrie, Surf. Sci. **320**, 25 (1994).  
<sup>6</sup>P.A. Cox and A.A. Williams, Surf. Sci. **152/153**, 791 (1985).  
<sup>7</sup>C.A. Ventrice, T. Bertrams, H. Hannemann, A. Brodde, and H. Neddermeyer, Phys. Rev. B **49**, 5773 (1994).  
<sup>8</sup>K. Koike and T. Furukawa, Phys. Rev. Lett. **77**, 3921 (1996).  
<sup>9</sup>W. Ranke, M. Ritter, and W. Weiss, Phys. Rev. B **60**, 1527 (1999).  
<sup>10</sup>S.A. Flodstrom and C.W.B. Martinsson, Surf. Sci. **118**, 513 (1982).  
<sup>11</sup>*Handbook of Auger Electron Spectroscopy*, 2nd ed. (Perkin-Elmer, Eden Prairie, 1976).  
<sup>12</sup>Error is estimated from the assumed precision of the technique (atomic ratio determined by AES: 20%, lattice constant determined by RHEED: 1%).  
<sup>13</sup>M. Kiguchi, T. Goto, K. Saiki, T. Sasaki, Y. Iwasawa, and A. Koma, Surf. Sci. **512**, 97 (2002).  
<sup>14</sup>K. Saiki, Y. Nakamura, and A. Koma, Surf. Sci. **269/270**, 790 (1992).  
<sup>15</sup>V.E. Henrich, G. Dresselhaus, and H.J. Zeiger, Phys. Rev. Lett. **36**, 158 (1976).  
<sup>16</sup>K. Nishita, K. Saiki, and A. Koma, Appl. Surf. Sci. **169/170**, 180 (2001).  
<sup>17</sup>K. Ueno, Y. Uchino, K. Iizumi, K. Saiki, and A. Koma, Appl. Surf. Sci. **169/170**, 184 (2001).  
<sup>18</sup>*The Surface Science of Metal Oxides*, edited by V. E. Henrich and P. A. Cox (Cambridge University Press, Cambridge, 2000), p. 136.  
<sup>19</sup>M. Kiguchi, R. Arita, G. Yoshikawa, Y. Tanida, M. Katayama, K. Saiki, A. Koma, and H. Aoki, Phys. Rev. Lett. **90**, 196803 (2003).